

Supporting Information
for
Development of a Spectrophotometric Assay for
High-Throughput Screening and Mechanistic
Characterization of Glucose-1-Phosphate
Thymidyltransferase Inhibitors

Bronwyn E. Rowland[†], Jesse C. Fuller[†], David L. Jakeman^{†‡}*

[†] Department of Chemistry, Dalhousie University, Halifax, Nova Scotia, B3H 4R2, Canada.

[‡] College of Pharmacy, Dalhousie University, Halifax, Nova Scotia, B3H 4R2, Canada.

* Author to whom correspondence should be addressed.

email: David.jakeman@dal.ca

TABLE OF CONTENTS

Table S1. Oligonucleotide primers used for site-directed mutagenesis.	3
Figure S1. Gel electrophoresis of wt Cps2L and the E253D variant.....	3
Figure S2. Quantifying total phosphate concentration using the malachite green assay	4
Scheme S1. Activation of α -PGM-by α -D-fructose-1-6-bisphosphate to generate α -D-glucose-1,6-bisphosphate.....	4
Figure S3. Representative progress curves for determining Cps2L kinetic parameters	5
Figure S4. Representative TDP-Rha reactions in the absence of Cps2L.....	5
Figure S5. TDP-Rha binding at α -D-glucose-1-phosphate thymidyltransferase allosteric sites. 6	
Figure S6. Effect of Mg^{2+} on <i>L. mesenteroides</i> G6PD	6
REFERENCES	7

Table S1. Oligonucleotide primers used for site-directed mutagenesis.

Primer type	Oligonucleotide primer ^a	Translational change	T _m (°C)
forward	5'-CAATTTGGAAGATATCGCCTATCG-3'	E253D	60
reverse	5'-GCAACTTGAACGTTTTGCATG-3'	N245N	59

^aThe altered codons are underlined and the specific nucleotide substitutions are shown in boldface.

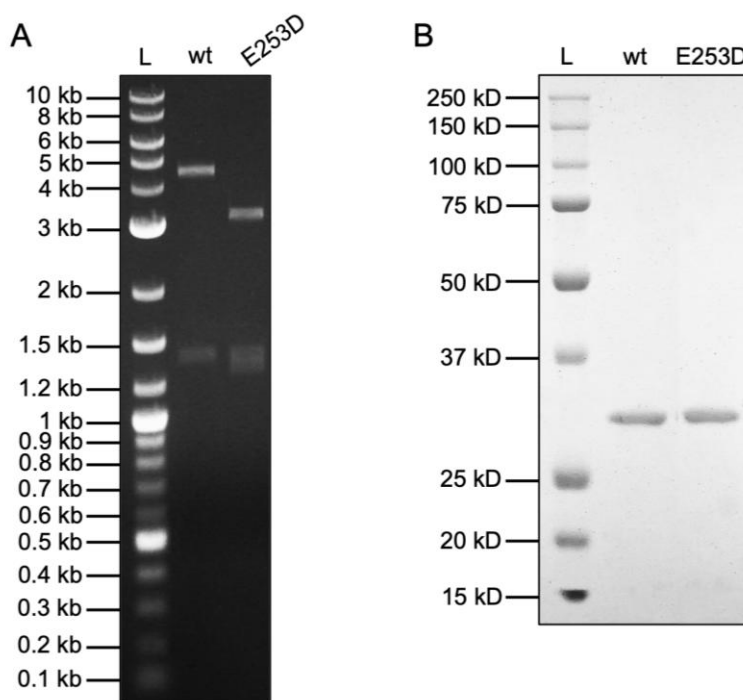


Figure S1. Gel electrophoresis of wt Cps2L and the E253D variant. (A) Plasmids bearing wt and E253D Cps2L variant sequences were digested with AclI and visualized by gel electrophoresis using a 1.2% agarose gel with RedSafe nucleic acid staining solution. Lane L is the DNA molecular weight ladder. Bands at 4427 kb, 1368 kb, and 396 kb (low resolution) reflect a non-mutated DNA sequence, as seen in the wt Cps2L lane. Bands at 3145 kb, 1368 kb, 1282 kb, and 396 kb (low resolution) reflect a mutated DNA sequence, as seen in the Cps2L E253D lane. (B) Purified wt Cps2L and Cps2L E253D protein were visualized by SDS-PAGE using a 4% acrylamide stacking gel and a 12.5% acrylamide resolving gel, stained with Coomassie Brilliant Blue G-250. Lane L is the protein molecular weight ladder. The expected molecular weight for both proteins is approximately 34.4 kDa.

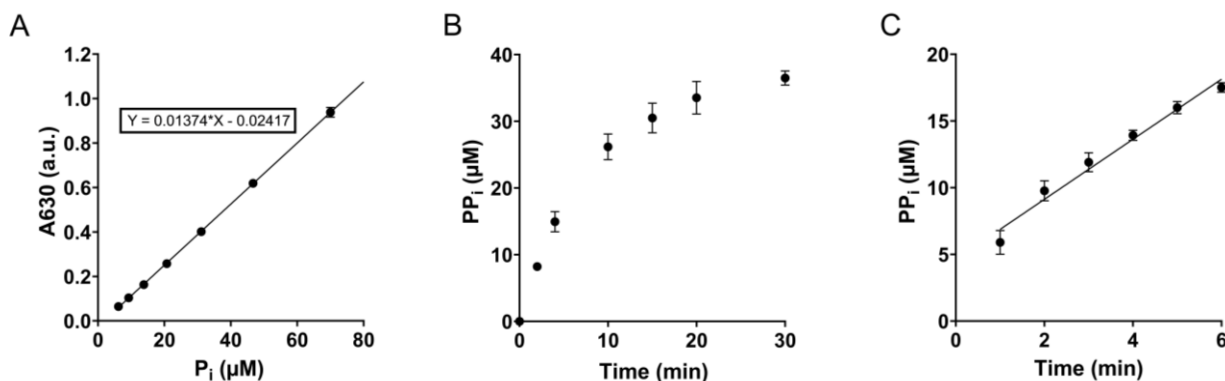
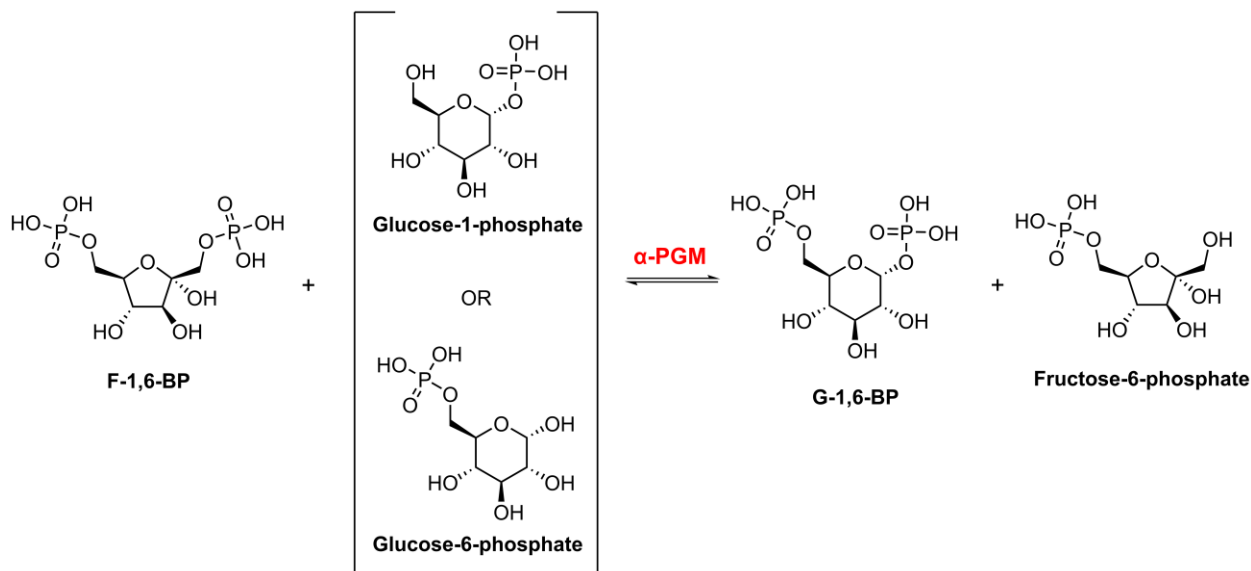


Figure S2. Quantifying total phosphate concentration using the malachite green assay. (A) Representative monophosphate standard curve. Two 1.5-fold serial dilutions of P_i (70 μM to 6.15 μM) were prepared in assay buffer. Absorbance at 630 nm was measured, normalized to a buffer control (0 μM P_i), averaged across replicates, and then fit by linear regression. Data shown are mean \pm SD ($n=2$), although error bars are smaller than the data points. (B) Cps2L activity over time, monitored by the production of PP_i over 30 minutes, quantified using the monophosphate standard curve. PP_i production is equimolar to TDP-Glc production. (C) Linear product formation was observed between 1-6 min. Reactions contained 10 nM Cps2L, 100 μM TTP, 100 μM G-1-P, 5 mM MgCl_2 , and 0.8 EU/mL IPP, and were quenched with 0.1% formic acid. Data shown are mean \pm SD ($n=2$).

Scheme S1. Activation of α -PGM-by α -D-fructose-1-6-bisphosphate to generate α -D-glucose-1,6-bisphosphate.^a



^a α -D-fructose-1-6-bisphosphate (F-1,6-BP) phosphorylates the α -PGM catalytic serine. This phosphoryl group is enzymatically transferred to α -D-glucose-6-phosphate or α -D-glucose-1-phosphate to produce α -D-glucose-1,6-bisphosphate (G-1,6-BP).¹

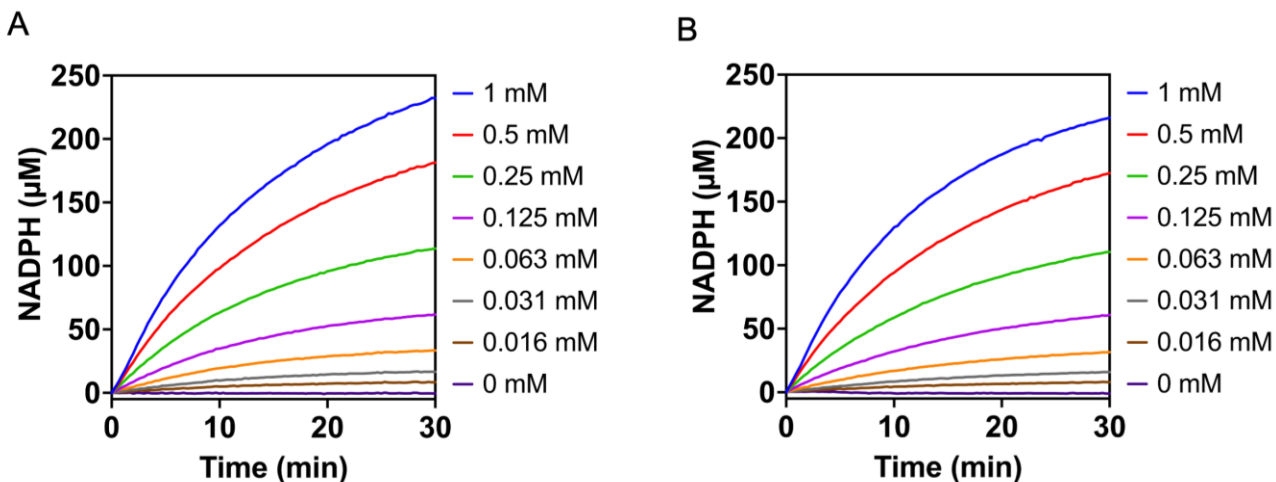


Figure S3. Representative progress curves for determining Cps2L kinetic parameters. (A) Cps2L activity was measured across a 2-fold serial dilution of UDP-Glc using the developed NADPH-coupled assay (0.5 mM PP_i, 1 mM NADP⁺, 100 μM F-1,6-BP, 5 mM MgCl₂, 1.5 EU/mL PGM, 1.5 EU/mL G6PD, and 25 nM Cps2L, monitored at 340 nm). Activity was also measured in the absence of UDP-Glc, but this v_i was not used to fit the Michaelis-Menten plot. (B) Cps2L activity was measured across a 2-fold serial dilution of PP_i using the developed NADPH-coupled assay (0.5 mM UDP-Glc, 1 mM NADP⁺, 100 μM F-1,6-BP, 5 mM MgCl₂, 1.5 EU/mL PGM, 1.5 EU/mL G6PD, and 25 nM Cps2L, monitored at 340 nm). Activity was also measured in the absence of PP_i, but this v_i was not used to fit the Michaelis-Menten plot.

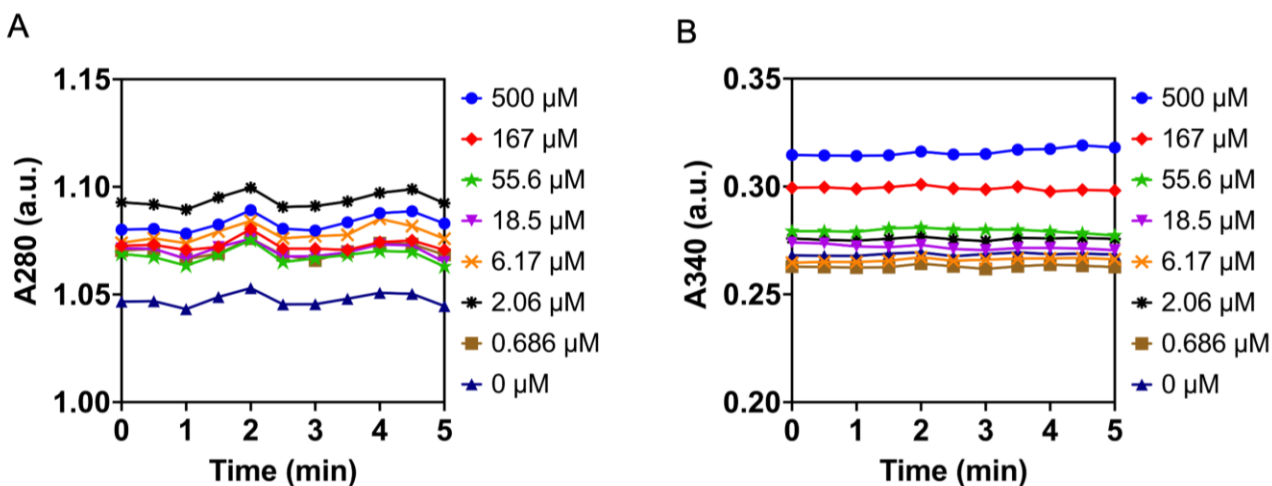


Figure S4. Representative TDP-Rha reactions in the absence of Cps2L. The absorbance of reaction mixtures containing all components of the NADPH-coupled assay (300 μM UDP-Glc, 100 μM PP_i, 500 μM NADP⁺, 100 μM F-1,6-BP, 8 mM MgCl₂, 1.5 EU/mL PGM, 1.5 EU/mL G6PD) except Cps2L were measured at (A) 280 nm and (B) 340 nm across a 3-fold serial dilution of TDP-Rha. No meaningful change in absorbance was measured over time at either wavelength (photometric accuracy for microplates in the SpectraMax Plus 384 UV/Vis microplate reader is $\pm 0.006 \text{ OD} \pm 1.0\%$ from 0-2 OD).²

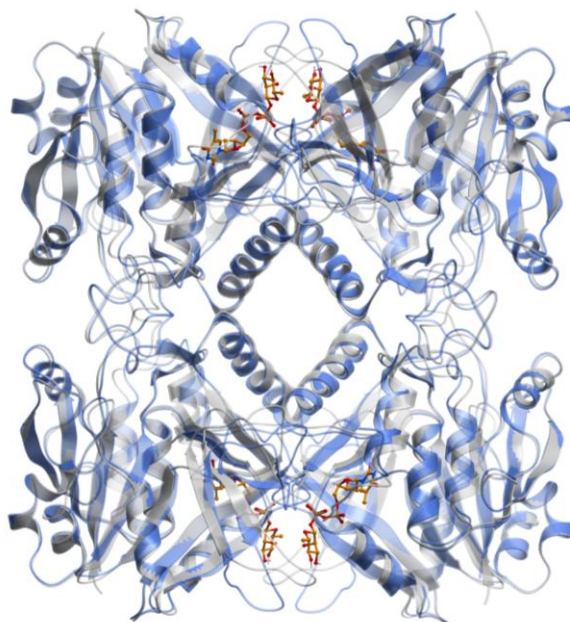


Figure S5. TDP-Rha binding at α -D-glucose-1-phosphate thymidyltransferase allosteric sites. The tertiary structure of *S. pneumoniae* Cps2L was predicted using AlphaFold3 (blue) and aligned to the crystal structure of *P. aeruginosa* RmlA (grey, PDB: 1G3L).³ The homologs share a common fold and have high sequence similarity (68%). TDP-Rha molecules located in the *P. aeruginosa* RmlA allosteric sites are shown in yellow.

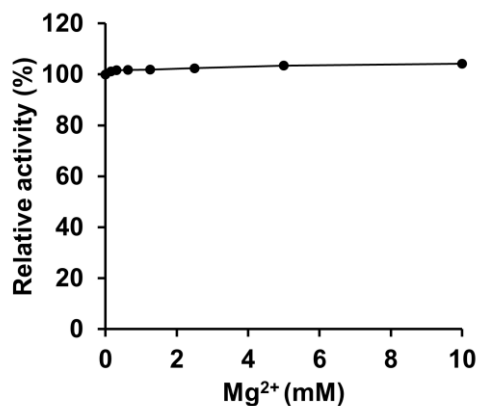


Figure S6. Effect of Mg²⁺ on *L. mesenteroides* G6PD. Relative activity represents the percent ratio of each measured v_i to that of the maximum observed v_i in the dataset. Reactions contained 0.01 EU/mL G6PD, 100 μ M NADP⁺, 500 μ M G6P, and 0-10 mM Mg²⁺ in 40 mM MOPS buffer. G6PD activity was minimally affected by Mg²⁺ concentration.

REFERENCES

- 1 J. V. Passonneau, O. H. Lowry, D. W. Schulz and J. G. Brown, *J. Biol. Chem.*, 1969, **244**, 902–909.
- 2 SpectraMax Plus 384 Microplate Reader,
<https://www.moleculardevices.com/sites/default/files/en/assets/data-sheets/br/spectramax-plus-384-microplate-reader.pdf>.
- 3 W. Blankenfeldt, M. Asuncion, J. S. Lam and J. H. Naismith, *EMBO J.*, 2000, **19**, 6652–6663.